Journal of Alloys and Compounds 509 (2011) 1749–1755

Contents lists available at ScienceDirect

Journal of Alloys and Compounds

journal homepage: www.elsevier.com/locate/jallcom

Devitrification behavior and some electrical properties of GeSeTl chalcogenide glass

E. Abd El-Wahabb*, M.M. Abd El-Aziz, E.R. Sharf, M.A. Afifi

Faculty of Education, Physics Department, Ain Shams University, Roxy, Cairo, Egypt

ARTICLE INFO

Article history:
Received 12 March 2010
Received in revised form 5 October 2010
Accepted 10 October 2010
Available online 21 October 2010

Keywords:
Devitrification
Electrical properties

ABSTRACT

The activation energy of crystallization E_c of $GeSe_3Tl_{0.3}$ and $GeSe_4Tl_{0.3}$ chalcogenide glasses was calculated from the shift of the DTA exothermic peaks with changing the heating rate. Values of E_c were calculated by different methods and it was found that it decreases with increasing Se content.

Amorphous thin films of the present glasses were prepared using thermal evaporation technique. Electrical conductivity and *I–V* characteristics have been studied at temperatures below the glass transition temperature T_g and over a wide range of thickness (57.4–680 nm). The dc conductivity was linear in the Arrhenius Plot in the considered temperature range and increases with the increase of Se content. The activation energy for the dc conduction ΔE_σ is decreased with increasing Se content and film thickness. The observed compositional dependence of ΔE_σ has been correlated with the increase of weak Se–Se bond density at the expense of strong Ge–Se bond density. *I–V* characteristic curves indicates the memory type switching phenomenon for these compositions and it is explained in accordance with the electrothermal model initiated from Joule heating of a current channel.

1. Introduction

Chalcogenide glasses have been attracting much attention in the field of electronics as well as in infrared optics, since they exhibit several peculiar phenomena useful for devices such as electrical switches, memories, image storage, and photo resistors. Addition of thallium to chalcogenide glasses is generally accompanied by marked changes in their structural and physical properties [1–4]. The system GeSeTl is considered to be one of the new generation of chalcogenide glasses. Therefore, a lot of work has been done on impurities effect on conductivity and optical properties [5–8]. The glass formation region in the GeSeTl system has been reported for the materials prepared by air-quenching [9,10] and those prepared by ice-water quenching [11] techniques.

Dc, ac electrical conductivity, switching phenomenon and optical properties of GeSeTl system in thin films form were studied by many others [1,3,8,12,13].

It is intended in this work to study the structure transformation, the effect of thickness and Se content on the dc electrical properties and on the switching phenomenon in GeSeTl amorphous thin films.

2. Experimental details

The bulk glasses of GeSeTl system were prepared by direct mono temperature synthesis. The appropriate quantities of highly pure Ge, Se and Tl (5N) requiring 10 g of each composition were charged together into a dry, clean silica tube. The charged tube was sealed under a vacuum of 10^{-5} Torr.

Synthesization was carried out in an oscillatory furnace in the following sequence: The temperature was first raised to 523 K and kept constant for about 1 h. The temperature was then raised up to 673 K and kept at this temperature for about 2 h. Finally the temperature was raised to 1223 K and kept at this temperature for 6 h. During heating the charged tube was shaken to ensure the homogeneity of the composition. Then, the tube was suddenly quenched in ice cold water.

Thin films of the GeSeTl glassy system were prepared by thermal evaporation technique using a coating unit (Edward E-306 A) on dry, clean, highly polished glass and pyrographite substrates for electrical and switching measurements respectively. These films were deposited under vacuum of 10^{-5} Torr at room temperature and the deposition parameters were kept almost the same for all the samples. The thickness of these films was controlled during deposition by using a quartz crystal thickness monitor and then measured by Tolansky's method of multiple beam Fizeau fringes [14].

The amorphous nature of the resulting GeSeTl thin films were verified by the absence of any diffraction lines in their X-ray patterns.

The chemical composition of the obtained films was checked by energy dispersive X-ray analysis EDX using scanning electron microscope (JEOL-JSM 5400) with EDX unit (Oxford). Finally quantative analysis results were obtained from the spectra by processing the data through the ZAF correction program. It was found that the two compositions under investigation were $GeSe_3Tl_{0.3}$ and $GeSe_4Tl_{0.3}$.

A micro DTA apparatus of a Shimadzu DT-30 model was used for the thermal analysis. The general features of the thermograms are: The glass transition temperature T_g that detect the temperature range of investigation, the crystallization temperature T_c, and the melting point T_m.

For electrical conductivity measurements, thin films of the present compositions were sandwiched between two Al electrodes. The electrical resistance (R) of samples was measured using a digital electrometer (Keithley, Model 616A) and then the conductivity was deduced. The temperature was measured by digital thermometer.

To study the *I–V* characteristics, thin film samples were evaporated onto highly clean and polished pyrographite substrates, and then sandwiched between two electrodes. The upper electrode was movable with its lower part made of plat-

* Corresponding author.
E-mail address: e_wahabb@hotmail.com (E. Abd El-Wahabb).

0925-8388/$ – see front matter © 2010 Elsevier B.V. All rights reserved.
doi:10.1016/j.jallcom.2010.10.033

Table 1
Values of T_g, T_c, T_m and T_g/T_m for the two compositions under investigation.

Compositions	Rate α, °C/min	T_g, K	T_c, K		T_m, K	T_g/T_m
			T_0 begin	T_p peak		
$GeSe_3Tl_{0.3}$	5	457	536	552	615	0.743
	10	–	539	553	616	–
	20	463	541	580	643	0.720
	30	459	553	591	641	0.716
$GeSe_4Tl_{0.3}$	5	435	550	563	612	0.711
	10	433	555	578	616	0.703
	20	440	568	588	613	0.718
	30	–	573	593	618	–

inum needle of 0.2 mm diameter, and the lower electrode was a circular brass disk. The measuring cell [15] was introduced in a simple electrical circuit provided with the above mentioned electrometer to measure the potential drop across the studied sample and a microdigital multimeter (TE 924) to measure the current passing through the sample.

3. Results and discussion

3.1. Structural identification

X-ray diffraction carried out for the investigated GeSeTl systems in thin film form are shown in Fig. 1. It is characterized by the absence of any diffraction line, indicating the amorphous nature of the prepared thin films.

DTA thermograms of $GeSe_3Tl_{0.3}$ and $GeSe_4Tl_{0.3}$ amorphous compositions were recorded at the heating rates 5, 10, 20 and 30 °C/min and shown in Fig. 2a and b respectively. Each of these thermograms is characterized by endothermic peak corresponding to the glass transition temperature T_g, one exothermic peak denoting the crystallization temperature T_c and one endothermic peak denoting the melting temperature T_m. Values of transition temperatures T_g, T_c (T_0 begin, T_p peak) and T_m are listed in Table 1. Also, the values of T_g/T_m are listed in Table 1.

It is observed that values of T_g and T_m are nearly independent of the heating rate α, while T_c changes markedly with α.

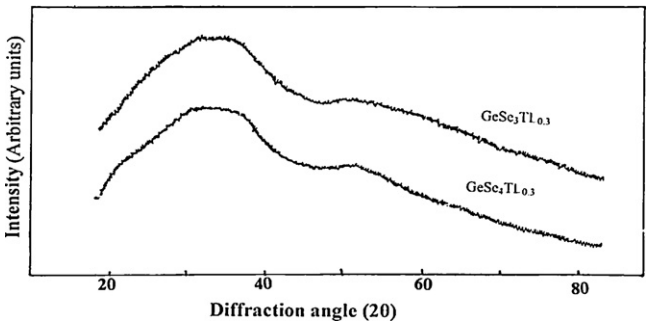

Fig. 1. X-ray diffraction patterns for $GeSe_3Tl_{0.3}$, and $GeSe_4Tl_{0.3}$ thin films.

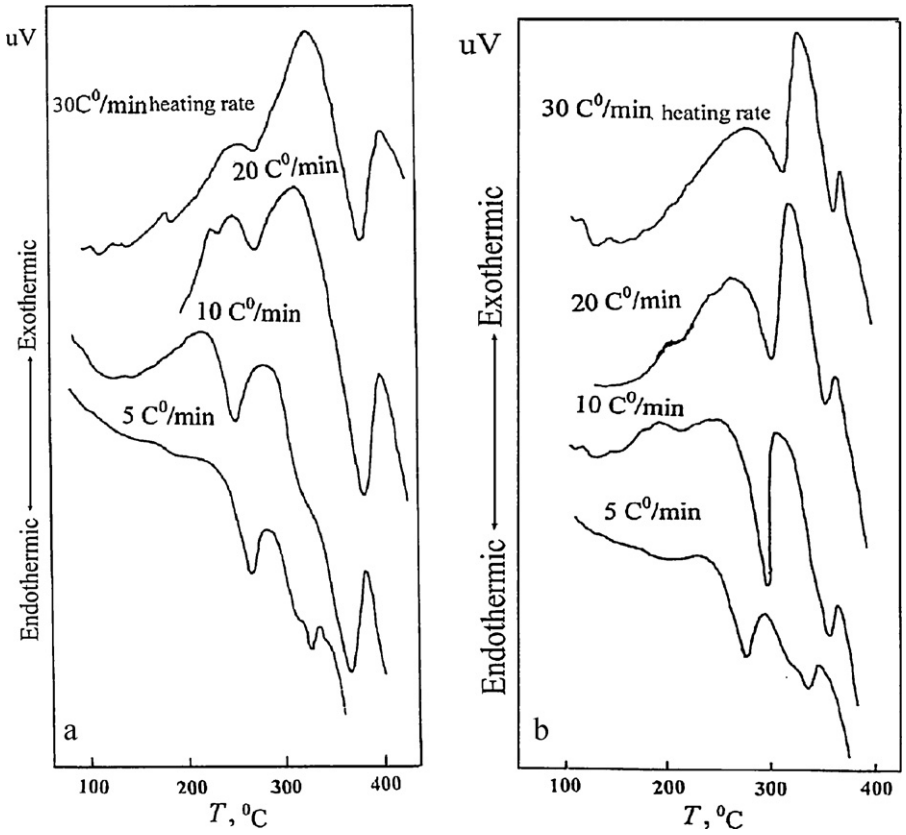

Fig. 2. Differential thermal analysis DTA at different heating rate of (a) $GeSe_3Tl_{0.3}$ and (b) $GeSe_4Tl_{0.3}$ compositions.

Values of T_g fluctuates around a mean value as α change because the relaxation time of the glass transition process is small compared with the time allowed by various heating rate. Consequently, one should not expect that the heating rate have a strong effect on the peak of T_g. The decrease of T_g with composition as shown in Table 1 can be understood using the chemically ordered network (CON) model by considering the chemical bond energies. This model is commonly used for explaining the features observed in the compositional dependence of various properties in chalcogenide glasses. The bond energies for Se–Se = 44, Ge–Ge = 37.6 and Ge–Se = 49.4 kcal/mole were calculated using Pauling's equation [16]. Accordingly with the increase of Se content, the Ge–Se bonds will be replaced by Se–Se bonds which have lower bond energy of 5.4 kcal (mole)$^{-1}$ thus, the glass transition temperature decreases.

The activation energy of crystallization E_c for GeSeTl systems under investigation have calculated from the shifts of the DTA exotherms, T_p which defined as the temperature of maximum crystallization rate with the heating rate α that observed in Fig. 2a and b by applying three methods.

1. According to Kissinger [17]

$$\ln\left(\frac{\alpha}{T_p^2}\right) = \text{const.} - \frac{E_c}{KT_p} \quad (1)$$

K is the Boltzmann's constant. Fig. 3a shows the plot of $\ln\left(\alpha/T_p^2\right)$ versus $(1/T_p)$ for the exotherms of Fig. 2a and b for $GeSe_3Tl_{0.3}$ and $GeSe_4Tl_{0.3}$ compositions. E_c was calculated from the slope of straight lines and the obtained value is shown in Table 2.

2. Ozawa's method

According to Ozawa's equation [18,19]

$$\ln\alpha = \text{const.} - 1.052\frac{E_c}{KT_p} \quad (2)$$

A plot of $\ln\alpha$ as a function of $1/T_p$ for the investigated compositions is illustrated in Fig. 3b. It is observed that it yields a straight line from the slop of which, E_c was calculated for each composition and given in Table 2.

3. Method of Augis and Bennett

Augis and Bennett [20] developed an accurate method in which

$$\ln\left[\frac{\alpha}{T_p - T_0}\right] \cong \ln K_0 - \frac{E_c}{KT_p} \quad (3)$$

K_0 is the frequency factor for crystallization. The activation energy for crystallization E_c is deduced using Eq. (3) from the plot of $\ln[\alpha/(T_p - T_0)]$ versus $1/T_p$ as shown in Fig. 3c. Values of E_c and K_0 for amorphous $GeSe_3Tl_{0.3}$ and $GeSe_4Tl_{0.3}$ have been calculated and are given in Table 2.

From Table 2, it is observed that values of E_c obtained by the above mentioned three methods are approximately of the same order for each composition. Also, it is obvious that E_c decreases with increasing the Se content which causes the reduction of the amorphous phase i.e. decreases the degree of chemical disorder and leads to the increase of crystallization process.

This suggestion was confirmed by ratio T_g/T_m that decreases with the increase of Se content, since, according to Turnbull [21], the effect of increasing the ratio T_g/T_m is to decrease the rate of nucleation and leads to the decrease of crystallization rate. This effect has been also observed for previous work of GeSeTl glasses [22–25].

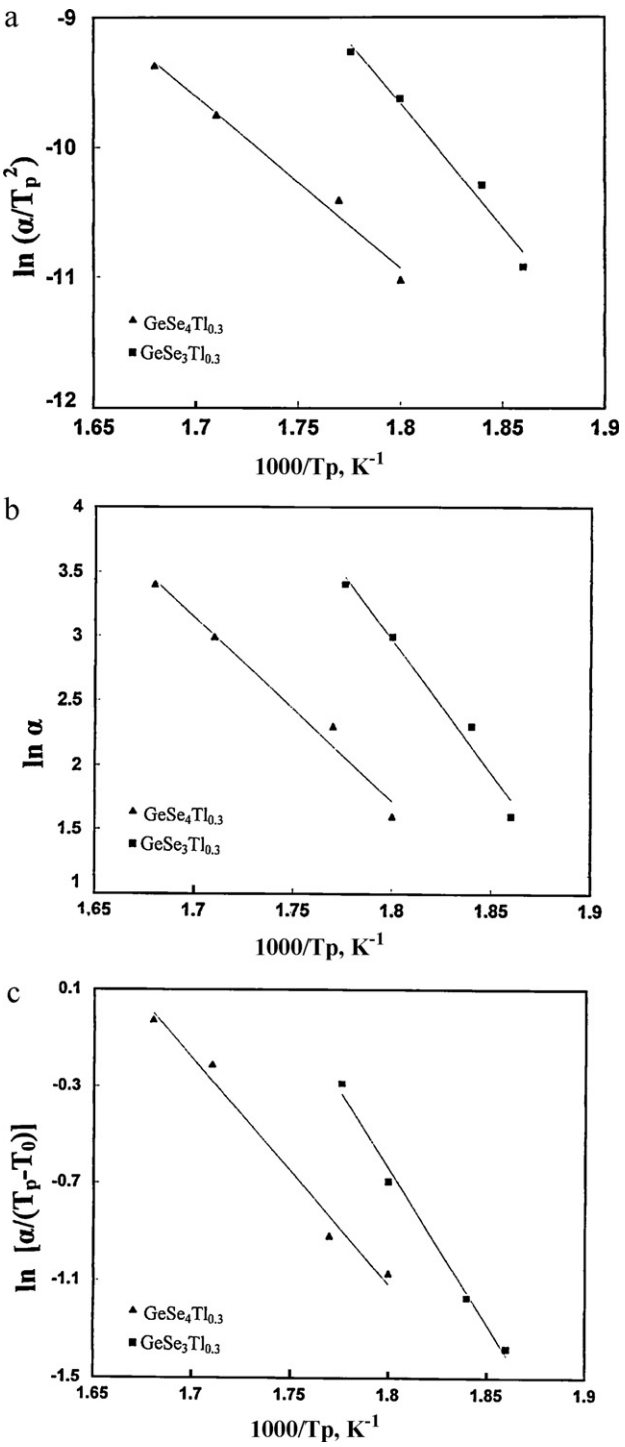

Fig. 3. (a) A plot of $\ln(\alpha/T_p^2)$ versus $1000/T_p$ for $GeSe_3Tl_{0.3}$ and $GeSe_4Tl_{0.3}$ compositions. (b) A plot of $\ln\alpha$ versus $1000/T_p$ for $GeSe_3Tl_{0.3}$ and $GeSe_4Tl_{0.3}$ compositions. (c) A plot of $\ln[\alpha/(T_p - T_0)]$ versus $1000/T_p$ for $GeSe_3Tl_{0.3}$ and $GeSe_4Tl_{0.3}$ compositions.

3.2. Dc electrical properties

To study the effect of composition on the dc electrical properties, thin films of $GeSe_3Tl_{0.3}$ and $GeSe_4Tl_{0.3}$ with nearly the same thickness (333, 330 nm) were used. The variation of dc conductivity as a function of temperature was studied in the range (303–403 K) and illustrated in Fig. 4 as a relation between $\ln\sigma_{dc}$ versus T^{-1} for the two compositions.

Table 2
Values of the activation energy of crystallization E_c that obtained by different methods for the two compositions under investigation.

Composition	Kissinger's method	Ozawa's method	Method of Augis and Bennett	
	E_c (kJ/mole)	E_c (kJ/mole)	E_c (kJ/mole)	K_0 (s^{-1})
$GeSe_3Tl_{0.3}$	178.19	168.93	108.2	8.155×10^9
$GeSe_4Tl_{0.3}$	118.833	109.44	77.3	6.144×10^6

The plot suggests that there is one type of conduction mechanism contribute to the conductivity in the considered range of temperature. This indicates that $\sigma(T)$ exhibits activated temperature dependence in accordance with the relation,

$$\sigma = \sigma_0 \exp\left(\frac{-\Delta E_\sigma}{KT}\right) \quad (4)$$

σ_0 is the pre-exponential factor which depends on the charge carrier mobility and density of states, K Boltzmann's constant, T the absolute temperature and ΔE_σ is called the conduction activation energy.

Table 3 lists the values of ΔE_σ, σ_0 and σ_{RT} (the conductivity at room temperature ≈303 K) that estimated from Fig. 4 and Eq. (4) for both compositions. It is clear from this table and Fig. 4 that the increase in Se content leads to an increase in σ_0, σ_{RT} and σ, at any and a decrease in ΔE_σ. This is attributed to that the increase of Se in $GeSe_3Tl_{0.3}$ temperature increases Se–Se bond density at the expense of Ge–Se bond density. This increases the low bond density, since Se–Se bond energy is lower than that of Ge–Se. Consequently, the activation energy decreases and the electrical conductivity increases. The obtained values of ΔE_σ are in good agreement with earlier results for GeSeTl system [1,3,13].

To show the effect of thickness on the dc electrical properties, electrical conductivity σ_{dc} as a function of temperature for $GeSe_3Tl_{0.3}$ and $GeSe_4Tl_{0.3}$ films with different thickness in the range (57.4–333 nm) and (102–680 nm) respectively is depicted in Fig. 5a and b.

The obtained linear relations indicates that both compositions exhibits one type of conduction mechanism in the considered ranges of temperature and thickness explained as before. Values of ΔE_σ, σ_0 and σ_{RT} are calculated and given in Table 3.

It is clear from Fig. 5 and Table 3, that ΔE_σ, σ_0, σ_{RT} and σ decrease with the increase of film thickness at any temperature for both investigated compositions. The decrease of electrical conductivity with increasing the film thickness is explained according to Mott and Davis [26] model involving the presence of localized states originating from the lack of long range order and extending into the mobility gap, such that each of them activates the motion of carriers within a given range of temperature.

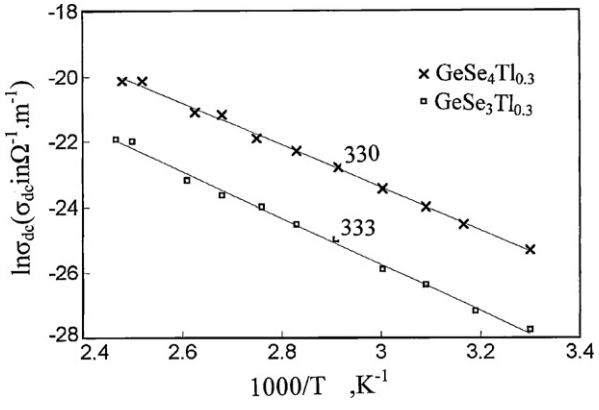

Fig. 4. The electrical conductivity of $GeSe_3Tl_{0.3}$ (333 nm) and $GeSe_4Tl_{0.3}$ (330 nm) thin films as a function of temperature.

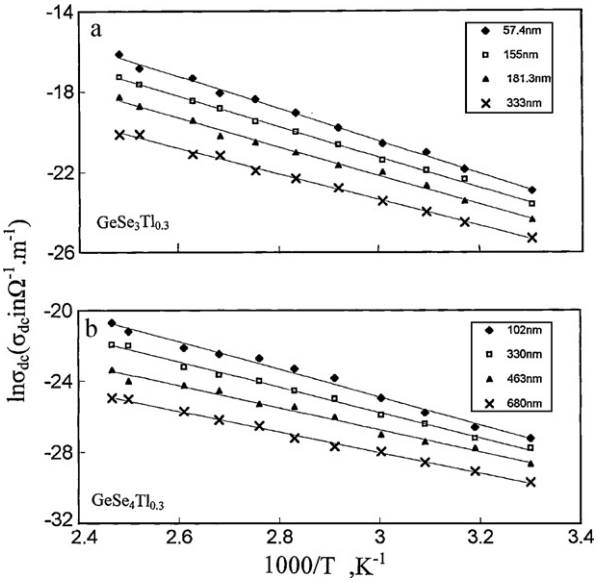

Fig. 5. The electrical conductivity as a function of temperature for (a) $GeSe_3Tl_{0.3}$ and (b) $GeSe_4Tl_{0.3}$ films with different thicknesses.

3.3. Switching properties

3.3.1. Static and dynamic I–V characteristics

Static and dynamic I–V characteristics curves were obtained for $GeSe_3Tl_{0.3}$ and $GeSe_4Tl_{0.3}$ thin films deposited on pyrographite substrates. The dynamic I–V characteristic curve displayed on the screen of a cathode ray oscilloscope using an ac source, and the static curves were measured with a dc source.

Both dynamic and static I–V characteristic curves have three states, OFF state with high resistance, negative resistance state beyond the threshold voltage and the ON state with low resistance. This is a typical characteristic of a memory switching effect.

The room temperature static I–V characteristic curves obtained for two samples of nearly the same thickness (333 and 330 nm) for the two investigated compositions are illustrated in Fig. 6 as representative examples. It is observed that, increasing the applied voltage from zero to the point a, a small current passes through the

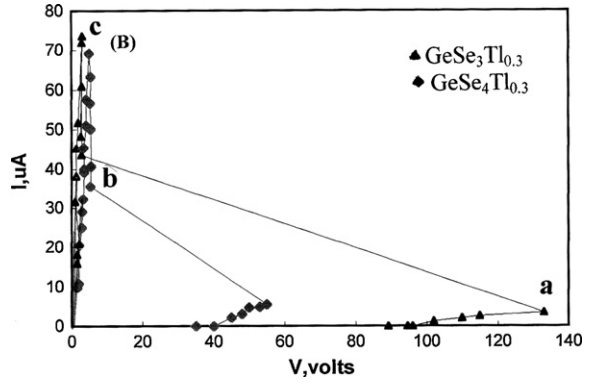

Fig. 6. Static I–V characteristic curve of $GeSe_3Tl_{0.3}$ (333 nm) and $GeSe_4Tl_{0.3}$ (330 nm).

Table 3
Effect of the composition and thickness on the values of ΔE_σ, σ_0 and σ_{RT} (30 °C).

Composition	Thickness (nm)	ΔE_σ (eV)	σ_0 $((\Omega\,m)^{-1})$	σ_{RT} (30 °C) $((\Omega\,m)^{-1})$
$GeSe_3Tl_{0.3}$	57.4	0.695	1.78×10^{-4}	2.29×10^{-12}
	155	0.653	7.61×10^{-5}	1.03×10^{-12}
	181.3	0.629	4.65×10^{-5}	6.25×10^{-13}
	333	0.613	3.79×10^{-5}	4.61×10^{-13}
$GeSe_4Tl_{0.3}$	102	0.673	4.46×10^{-2}	1.08×10^{-10}
	330	0.562	3.21×10^{-2}	3.37×10^{-11}
	463	0.531	2.73×10^{-2}	2.53×10^{-11}
	680	0.499	1.92×10^{-2}	1.69×10^{-11}

sample forming the first branch (oa) of the curve which represents the OFF state. At point (a) where the applied voltage equals a critical value (threshold voltage) $\overline{V_{th}}$, a sudden increase in the current and drop in the voltage to the point (b) takes place in a very short time of the order 10^{-9} s took place. Therefore, it is impossible to record any reading during this time [branch (ab)]. A further increase in the applied voltage increases the current without any significant increase in the potential drop [part (bc)] of the curve representing the ON state. On decreasing the applied voltage in this state, the current decreases until finally both become zero [part (co) of the curve].

3.3.2. Thickness and temperature dependence of the threshold voltage $\overline{V_{th}}$

The room temperature static *I–V* characteristic curves for $GeSe_3Tl_{0.3}$ and $GeSe_4Tl_{0.3}$ thin films with different thickness in the range (155–333 nm) and (330–680 nm) for the two compositions are illustrated in Fig. 7a and b respectively. The variation of the mean value of the threshold voltage $\overline{V_{th}}$ with the film thickness was studied and displayed in the insets of Fig. 7a and b.

It is clear that the obtained thickness dependence is linear in the range of study. The slope of the obtained line represents the mean value of the threshold field $\overline{E_{th}}$ (19.9×10^7 V/m for $GeSe_3Tl_{0.3}$ and 11.8×10^7 V/m for $GeSe_4Tl_{0.3}$).

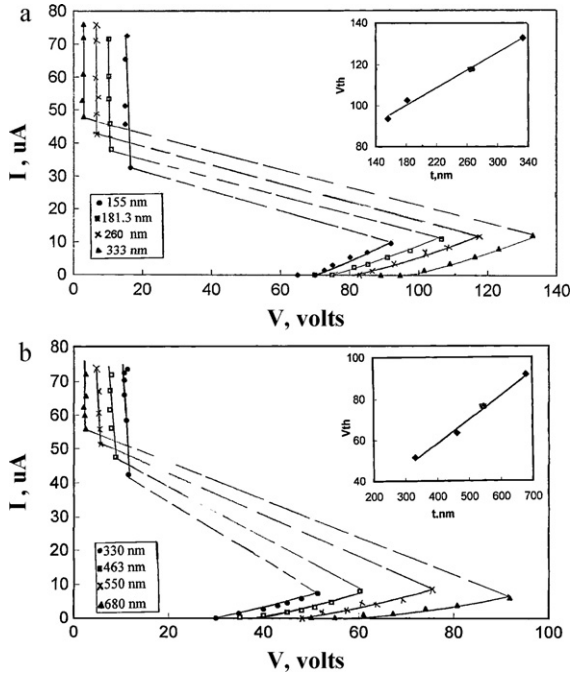

Fig. 7. Static *I–V* characteristic curves of (a) $GeSe_3Tl_{0.3}$ and (b) $GeSe_4Tl_{0.3}$ thin films of different thicknesses. The insets show thickness dependence of the mean threshold voltage for the above films.

I–V characteristics obtained at different temperatures in the range (303–403 K) for $GeSe_3Tl_{0.3}$ (t = 333 nm) and $GeSe_4Tl_{0.3}$ (t = 330 nm) thin film samples are represented in Fig. 8a and b respectively. The temperature dependence of the mean value of the threshold voltage $\overline{V_{th}}$ are illustrated in Fig. 9a and b for the two compositions respectively. It is clear from these figures that $\overline{V_{th}}$ seems to decreases exponentially with temperature. This relation plotted as $\ln\overline{V_{th}}$ versus $1000/T$ as shown in the insets of Fig. 9a and b. The obtained relation yielded a straight line satisfying the relation [27]

$$\overline{V_{th}} = V_0 \exp\left(\frac{\varepsilon}{KT}\right) \tag{5}$$

V_0 is constant and ε is threshold voltage activation energy. As shown from the insets of Fig. 9a and b, the obtained lines are nearly parallel indicating that the threshold voltage activation energy (ε) is single valued independent on sample thickness in the investigated range. The mean values of ε obtained from the slopes of the straight lines are 0.32 ± 0.002 eV for $GeSe_3Tl_{0.3}$ and 0.245 ± 0.002 eV for $GeSe_4Tl_{0.4}$.

The observed temperature dependence of the threshold voltage for the preswitching region can be explained in terms of an electrothermal model [27,28], since the temperature of the semiconductor is raised due to Joule-heating and the conduction process in an amorphous material is of an activated type [29], so, the conductivity of the sample will increases when heated. This will allow more current to flow through the heated region and allow more

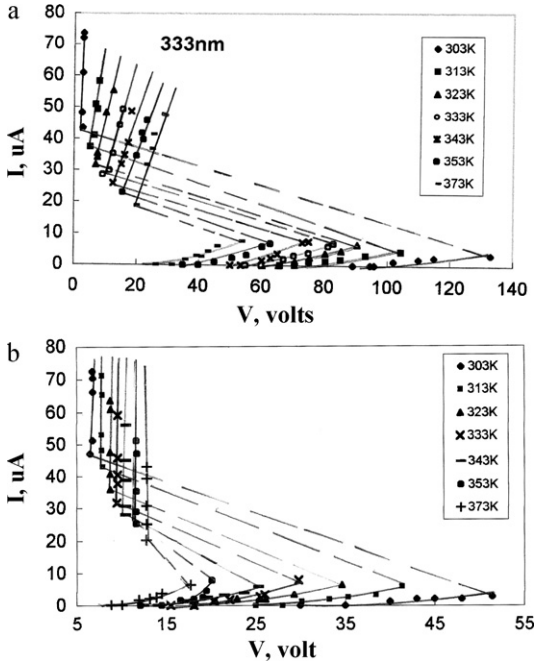

Fig. 8. *I–V* characteristic curves for (a) $GeSe_3Tl_{0.3}$ and (b) $GeSe_4Tl_{0.3}$ thin films at different temperatures.

Table 4
Values of $\Delta T_{breakdown}$ and ΔT for the investigated compositions at different temperatures as obtained from Eqs. (9) and (11).

Composition	t, nm	T, K	V_{th}, V	I_{th}, (A	$\Delta T_{breakdown}$, K	
					From Eq. (9)	From Eq. (11)
$GeSe_3TL_{0.3}$	333	303	133	3.4	14.19	57.18
		323	85.6	5.3	16.14	57.36
		343	54.6	8.4	18.2	57.99
		353	46.5	9.9	19.2	58.21
		373	33.1	14	21.5	58.59
$GeSe_4TL_{0.3}$	330	303	51.4	2.8	17.6	18.37
		323	33.8	4.4	20	18.98
		343	25.3	5.9	22.5	19.05
		353	20.1	7.9	23.9	20.27
		373	14.3	11.3	26.67	20.63

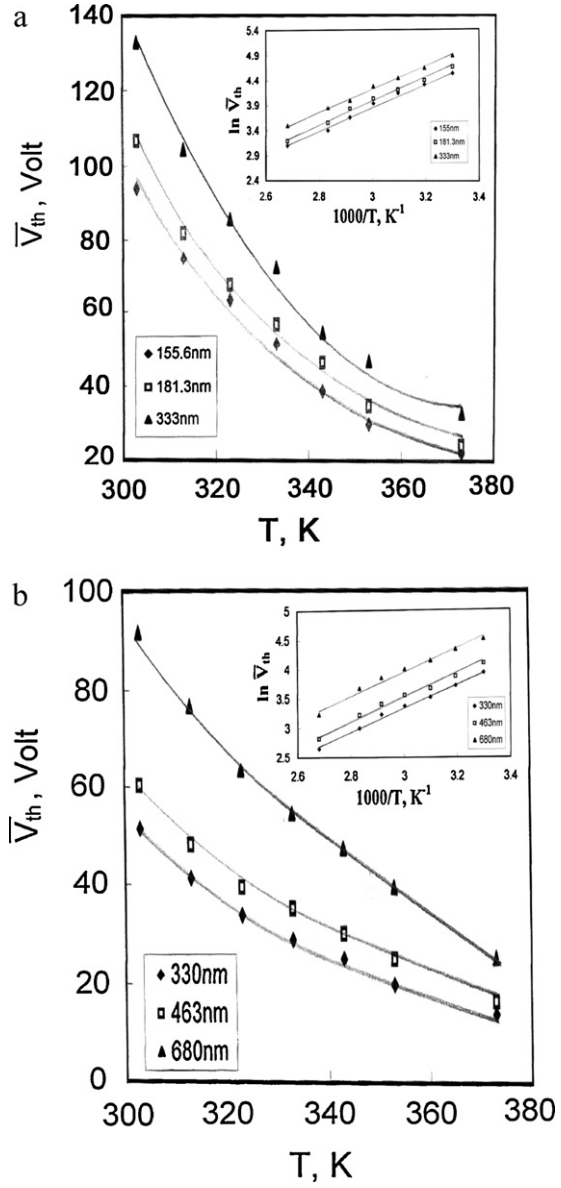

Fig. 9. Temperature dependence of the mean value of the threshold voltage $\overline{V_{th}}$ for (a) $GeSe_3Tl_{0.3}$ thin films of thicknesses (155, 181.3, 333 nm) and (b) $GeSe_4Tl_{0.3}$ thin films of thicknesses (330, 463, 680 nm). The insets show the plots of $\ln \overline{V_{th}}$ versus $1000/T$ for the above films.

Joule-heating, resulting in a further increase in the current density, ultimately. The temperature rise will become adequate to initiate a thermal breakdown owing to the strong temperature dependence of the conductivity. A stationary state is reached when the heat lost by conduction from the current filament becomes equal to the Joule-heat generated in that region.

The electrothermal model can be solved to a certain extent by finding a stationary state solution for the heat transport equation

$$C\left(\frac{dT}{dt}\right) = \sigma E^2 + \nabla(\psi \nabla T) \tag{6}$$

and the charge conservation equation:

$$-\left(\frac{1}{\sigma}\right)\left(\frac{dp}{dt}\right) = \nabla E \tag{7}$$

C is the heat capacity, ψ is the thermal conductivity, E the electric field intensity ($E = V_{th}/t$), σ the electrical conductivity of the sample which is given by Eq. (4) and p the charge density.

In the case of steady state breakdown, the time derivative of temperature (dT/dt) can be neglected for the solution of Eq. (6). Therefore, Eq. (6) can be expressed with the aid of Eq. (8) for a small temperature difference between the temperature at the middle of the specimen T_m and that of the surface T_s, ($\Delta T = T_m - T_s$) as follows [27]

$$8\psi\left(\frac{\Delta T}{d^2}\right) + \sigma E^2 = 0 \tag{8}$$

d is the sample thickness.

The steady state breakdown occurs when the amount of heat generated by Joule-heating cannot be removed by thermal conduction and the temperature difference necessary for breakdown can be obtained from Eqs. (6) and (8) in the form [27,30]

$$\Delta T_{\text{breakdown}} = \frac{T^2}{\Delta E_\sigma / K} \tag{9}$$

The temperature inside the active region of the specimen as a function of the power $Q = IV$ generated in it is given by the relation [31]

$$T = T_0 + \frac{Q}{2\pi\psi d} \tag{10}$$

$\Delta T = T - T_0$, T_0 is the ambient temperature. That is

$$\Delta T_{\text{breakdown}} = \frac{I_{th}V_{th}}{2\pi\psi d} \tag{11}$$

Table 4 gives the values of $\Delta T_{\text{breakdown}}$ that calculated from Eqs. (9) and (11) at different temperatures considering $\psi = 3.78$ W/m K [1,32] for the two investigated compositions with nearly the same thickness. From this table, it is appeared that values of $\Delta T_{\text{breakdown}}$ obtained from Eq. (9) are in the same order of magnitude as that obtained from Eq. (11). This supports the electrothermal model

for the switching process, and is in good agreement with previous results [1,32,33] for amorphous semiconducting thin films. Moreover, the agreement between the obtained values of $\varepsilon/\Delta E_\sigma$ and that obtained theoretically on the basis of the electrothermal model (0.5) [15] confirms also that the switching process for the two investigated compositions can be explained by the electrothermal model.

4. Conclusions

The activation energy of crystallization E_c calculated by different methods was found to decreases with increasing Se content.

Room temperature electrical conductivity σ_{RT} and the pre-exponential factor σ_0 increase, while the activation energy ΔE_σ decreases with the increase in Se content in the investigated compositions.

The values of ΔE_σ, σ_{RT} and σ_0 were found to decreases with increasing the film thickness for the two investigated compositions.

Dynamic and static *I–V* characteristic curves of thin films under investigation show typical memory switch. The measured switching characteristics ensure a likely activation character of the switching process. The mean value of the threshold voltage $\overline{V_{th}}$ increases linearly with increasing film thickness while it decreases exponentially with increasing temperature in the investigated ranges. Moreover, the observed phenomenon can be explained by electrothermal model of breakdown.

References

[1] M.F. Kotkata, et al., Thin Solid Films 240 (1994) 143.
[2] P. Pektov, C. Vodenicharov, C. Kanasitak, Phys. Status Solidi A 168 (1998) 447.
[3] M.M. Abd El-Raheem, J. Ovonic Res. 4 (6) (2008) 165–173.
[4] M.A. Afifi, M.M. Abd El-Aziz, H.H.M.F. Labib, E.G. El-Metwally, Vacuum 61 (2001) 45–53.
[5] Z.U. Borisovo, Conf. on Amorphous Semiconductor, vol. 80 (Kishinev, 1980).
[6] M.M. Abd El-Rahaem, J. Ovonic Res. 4 (6) (2008) 165–173.
[7] M.M. Abd El-Rahaem, J. Phys. Condens. Matter 19 (2007) 216209.
[8] M.M. Abd El-Raheem, M.M. Wakkad, N.M. Megahed, A.M. Ahmed, E.K. Shokr, J. Mater. Sci. 31 (1996) 5759.
[9] S.A. Demeovskii, Z.H. Neorgan, Khimi 13 (1968) 1721.
[10] Z.U. Borizova, L.P. Kornienko, A.A. Obraztsow, E. Yu Turkina, IZV. Akad. Nauk. SSR. Weorg. Mater. 12 (1976) 592.
[11] G. Parthasarathy, G.M. Naik, S. Asokan, J. Mater. Sci. Lett. 6 (181) (1987) 214.
[12] M.F. Kotkata, M.A. Afifi, H.H. Labib, N.A. Hegab, M.M. Abdel-Aziz, J. Phys. D. Appl. Phys. 27 (1994) 623.
[13] M. Zope, B.D. Muragi, J.K. Zope, J. Non-Cryst. Solids 103 (1988) 195.
[14] S. Tolaansky, Introduction to Interferometry, Longman, London, 1955.
[15] M.A. Afifi, N.A. Hegab, Vacuum 48 (1997) 135.
[16] R.A. Street, N.F. Mott, Phys. Rev. Lett. 35 (1975) 1293.
[17] H.E. Kissinger, Anal. Chem. 29 (1957) 1702.
[18] J.J. Zhang, R.F. Wang, H.M. Liu, J. Therm. Anal. Calorim. 66 (2001) 431.
[19] N.F. Mott, Phil. Mag. 19 (1969) 835.
[20] J.A. Augis, J.E. Bennett, J. Therm. Anal. 13 (1978) 283.
[21] D. Turnbull, Content Phys. 10 (1969) 473.
[22] M.M. Abdel-Aziz, M.A. Afif, H.H. Labib, E.G. El Metwally, Acta Physica Polonica A 98 (2000) 393.
[23] M.F. Kotkata, M.M. Radwan, M.H. El-Fouly, S.A. Fayek, J. Mater. Sci. 25 (1990) 2107.
[24] A.A. Abou-Sehely, Physica B 325 (2003) 372.
[25] C. Pacurariu, M. Lita, L. Lazau, D. Tita, G. Kovacs, J. Therm. Anal. Calorim. 72 (2003) 811.
[26] N.F. Mott, E.A. Davis, R.A. Street, Phys. Rev. Lett. 28 (1975) 813.
[27] R. Mehra, R. Shyam, P.C. Mathur, J. Non-Cryst. Solids 31 (1979) 435.
[28] H.J. Dewit, C. Creveccoeur, Solid State Electron. 15 (1972) 729.
[29] A.H. Abou El-Ela, N. Abdelmohsen, H.H. Labib, Appl. Phys. A (1981) 171.
[30] K. Shimawa, Y. Inagaki, T. Arizumi, Jpn. J. Appl. Phys. 12 (1973) 1043.
[31] T. Kaplan, D. Adler, J. Non-Cryst. Solids 8 (1972) 538.
[32] M.A. Afifi, N.A. Hegab, H.H. Labib, M. Fadel, Indian J. Pure Appl. Phys. 30 (1992) 211.
[33] M.A. Afifi, N.A. Hegab, A.E. Bekheet, Vacuum 47 (1996) 265.